Unsteady flowmeter

Eric Foucault, Philippe Szeger

Version of Record: https://www.sciencedirect.com/science/article/pii/S0955598618304382
Manuscript_2dd9aa2a45c4e24d8bf22ccf7d794e8e

Unsteady Flowmeter

Eric Foucault*, Philippe Szeger*

Institut Pprime, UPR 3346 CNRS - Université de Poitiers - ENSMA
6 rue Marcel Doré, TSA 41105
F86073 POITIERS Cedex 9, FRANCE

Abstract

An original method is presented to measure time resolved unsteady flow rate. From the kinetic energy theorem, the balance equation of the kinetic energy is integrated on a conical control volume (Venturi type). A non-linear ODE is obtained, simple enough to be resolved in real-time (that is to say in less than one time step). The two coefficients of the ODE depend only on the geometry of the device and are hence known by construction, it is therefore not necessary to calibrate the device. Experimental measurements at the intake of a combustion engine show that the device provides unsteady flow rate. By temporal integration, the unsteady measurements give a mean flow rate close to the reference flowmeter.

The same analysis is then applied to a cylindrical control volume with a singular pressure drop (induce by a grid for example). In this case, one of the two coefficients of the ODE must be determined experimentally. Experimental measurements carried out with this device at the intake of a combustion engine show that this second method follows the flow fluctuations. A good agreement is found between unsteady measurements integrated over a whole number of periods and reference mass flowmeter. The inversions of direction of the flow are taken into account by the prototype. This device, more compact than the conical version (Venturi type), allows real-time measurements of the unsteady flow rate.

Keywords: Unsteady flow rate, flowmeter, intake combustion engine, pulsating flow, backflow

*Corresponding author
Email addresses: eric.foucault@univ-poitiers.fr (Eric Foucault), philippe.szeger@univ-poitiers.fr (Philippe Szeger)

1. Introduction :

The flow measurement in pipes goes back to the origin of fluid mechanics and has remained one of a most common operations. There are virtually innumerable numbers of more or less advanced techniques for measuring average flow rates, but there are currently no flowmeters for time resolved measurements of unsteady flow rates. In a number of cases, only the mean flow rate is of interest to the user, either because more information is not useful to the process, or because it ignores the possibility of having access to unsteady flow rate. However it is necessary that the techniques used to measure the mean flow rate are not disturbed if there is also a more or less strongly unsteady velocity component. A large number of articles are devoted to this problem, and look at ways to prevent fluctuations from disturbing average measurements. (e.g. [1],[2], [3]).

Several ways have been proposed to access unsteady flow rate without having to spatially integrate spot velocity measurements. In case of pulsating laminar flows, authors [4, 5] have shown that for low frequencies ($\leq$ 1 Hz) the mass flow rate of the mean flow and that of the pulsating flow can be separated and both can be accurately measured.

It appears that it would be much better to measure the actual flow rate, even if it means to average it, than to try to measure only the continuous component of it. The purpose of this article is to propose a solution to measure the unsteady flow rate in a pipe.

Patents from 2005 and 2007 [6, 7] claim to be able to access the unsteady flow rate in a pipe from pressure drop. An ordinary differential equation (ODE) similar to Eq. (17) below is suggest without giving any justification.

This idea is taken up by Beaulieu *et al* [8] which show that this principle can be use to measure the pulsating flow rate that enters a mechanical breathing system with sufficient precision. However this does not justify the geometric constants A and B of Eq. (17). The results were experimentally validated and the prototype was tested using water. The velocity profiles were measured by particle image velocimetry (PIV) and the equipment was calibrated using an ultrasonic meter. The Venturi discharge coefficient was determined as a function of the Reynolds number for steady flows and pulsating flows of low frequencies ($\leq$ 4 Hz) with concurrence of the results.

Doblhoff-Dier *et al.*[9] also obtained time-resolved measurements using

orifice plates with an equation very similar to Eq. (17). They concluded that this equation might yield fair results as long as the ratio of the velocity pulsating component v' to $\omega d/2$ is no higher than 10. They argue that for higher ratios other effects, such as nonlinear impedance come into play. In spite of all the care brought to the pressure measurements, in particular to the tube connections and the phenomena of resonance, the bandwidth of their system was not sufficient for the higher modes of pulsation. This delicate point will be addressed below when describing the system. A recent review of pulsed flow measurements by orifices plates flowmeters can be found in Reis and Hanriot [10]. This shows that for low Reynolds number values at least,the inertial effects significantly affect the value of the discharge coefficient of the orifice plate, reducing the discharge values. It can be concluded in any case, orifice flowmeters, because of the recirculation they generate upstream and downstream of the orifice, are not good candidates for precise pulsated flow measurements.

Johnston *et al.*[11] have presented original measurement methods based on the wave propagation model to determine the flow rate using measured pressures as boundary conditions. Experiments have show that method with three transducers is robust and reliable but the implementation requires relatively long pipes length (typically several meters). This method must be further developed to allow the measurement of the mean flow rate and be relevant in turbulent regime.

The present work focuses on the measurement of unsteady flow in a pipe from a differential pressure measurement. First it is necessary to establish a differential equation allowing access to the unsteady flow rate in a pipe. This will show that the two constants A and B can be known by construction and that the proposed model therefore requires no calibration. Then two applications of the system are proposed: a flowmeter whose differential pressure is due to an increase in the flow velocity (Venturi type flowmeter) and a flowmeter whose differential pressure is due to a singular pressure drop (flowmeter with a grid). The system can extend to many other configurations using for example a pressure drop already present in the pipe where flow is to be known. The main applications targeted by this study are pulsated flows at the intake or exhaust of combustion engines.

Nomenclature

A, B	Flowmeter geometric parameters
r	Radial coordinate
R	Cylinder radius
Re	Reynolds number $= \frac{4q_m}{\pi D \mu}$
C	Head loss coefficient
D	Cylinder diameter
$\mathcal{D}$	Control volume
j	Imaginary unit $= \sqrt{-1}$
J_0	Zero order Bessel function of the first kind
N	Frequency
p	Pressure
q_m	mass flow rate
S	Cross-section area
t	Time
x	Axial coordinate
ΔP	Pressure difference (Pa)
Λ	Friction factor
μ	Fluid dynamic viscosity
ν	Fluid kinematic viscosity $= \frac{\mu}{\rho}$
ω	Pulsation $= 2\pi N$
ρ	Fluid density

Other symbols

$\Re(\ )$	Real part of complex quantity ()

2. Theorical framework:

A relationship between unsteady mass flow and the associated pressure drop is easy to find in pipe flow. The equation kinetic energy balance is well appropriated for this because it avoids the assumptions of non-viscosity and irrotational flow (c.f. [12], [13]).

2.1. Kinetic energy balance:

Application of the kinetic energy balance equation to Hagen-Poiseuille flow.

The kinetic energy balance is obtained by integrating, over a domain $\mathcal{D}$, the local form given by the kinetic energy theorem:

$$\underset{(I)}{\frac{\partial}{\partial t}\int_{\mathcal{D}} \frac{1}{2}\rho V^2 \, d\tau} + \underset{(II)}{\int_{\partial\mathcal{D}} \frac{1}{2}\rho V^2 (\overrightarrow{V}.\overrightarrow{n}) \, d\sigma} + \underset{(III)}{\int_{\partial\mathcal{D}} p(\overrightarrow{V}.\overrightarrow{n}) \, d\sigma} + \underset{(IV)}{\int_{\mathcal{D}} \overrightarrow{f}.\overrightarrow{V} \, d\tau} = \underset{(V)}{\int_{\partial\mathcal{D}} \overrightarrow{\tau}.\overrightarrow{V} \, d\sigma} - \underset{(VI)}{\int_{\mathcal{D}} \phi_1 \, d\tau} \qquad (1)$$

Thus, the temporal variation of kinetic energy over the domain $\mathcal{D}$, added to the kinetic energy and pressure flux across the boundaries of $\mathcal{D}$, is equal to the sum of the power of external viscous stresses exerted on $\partial\mathcal{D}$ and the power dissipated in $\mathcal{D}$ by viscosity.
This means that in inviscid flows, the temporal variation of kinetic energy in $\mathcal{D}$ is only due to the kinetic energy and pressure fluxes across the boundaries of $\mathcal{D}$. If the effects of viscosity are not negligible, it will be necessary to estimate them by experimental measurements.

It then remains to establish the conservation of kinetic energy in an axisymmetric domain (i.e. to write the conservation equation of the kinetic energy of a fluid motion in pipe of variable section).

2.2. Hypothesis:

1. motion generated by a unsteady longitudinal pressure gradient $P = p(x,t)$
2. one-dimensional flow: $\overrightarrow{V}(x,y,z,t) = V(x,y,z,t)\overrightarrow{x}$
3. no other volume force than gravity

4. negligible gravitational forces[1]: $\Omega = gz = 0$

2.3. Venturi type control volume:

Applying the relation (1) to the domain $\mathcal{D}$ defined in Fig. 1:

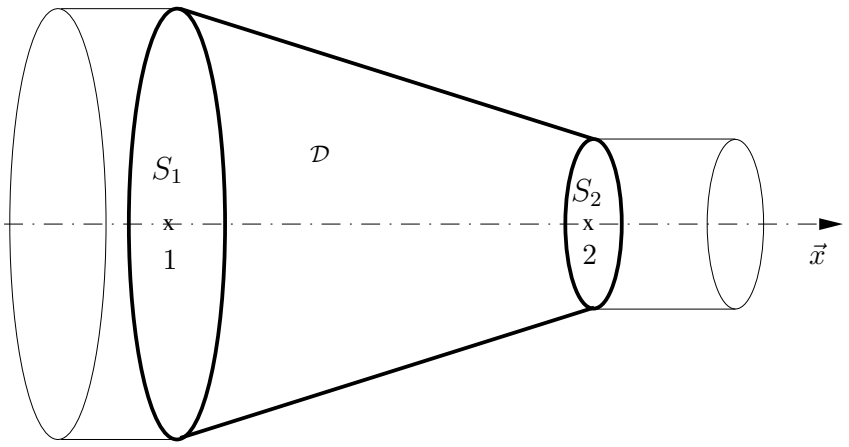

Fig. 1. Venturi type cylindrical pipe with axis $\vec{x}$ and cross-section $S(x)$.

$$\underset{(I)}{\frac{\partial}{\partial t}\int_{\mathcal{D}} \frac{1}{2}\rho V^2 \, d\tau} + \underset{(II)}{\int_{S_1 \cup S_2} \frac{1}{2}\rho V^2 (\overrightarrow{V}.\overrightarrow{n}) \, d\sigma} + \underset{(III)}{\int_{S_1 \cup S_2} p(\overrightarrow{V}.\overrightarrow{n}) \, d\sigma} = \underset{(V)}{\int_{S_1 \cup S_2} \overrightarrow{\tau}.\overrightarrow{V} \, d\sigma} - \underset{(VI)}{\int_{\mathcal{D}} \phi_1 \, d\tau} \quad (2)$$

Thus, these terms according to the mass flow $q_m(t)$ at the abscissa x:

$$\begin{aligned} q_m(t) = \rho(x,t) q_v(x,t) &= \rho(x,t) \int_{S(x)} \overrightarrow{V}(x,y,z,t).\overrightarrow{n} \, d\sigma \\ &= \rho(x,t) S(x) \overline{V}(x,t) \end{aligned} \quad (3)$$

[1] in fact this assumption is not essential, but is often verified.

Time variation of kinetic energy (I) :

The first term (I) of Eq. (2) becomes :

$$\begin{aligned}
\frac{\partial}{\partial t}\int_{\mathcal{D}} \frac{1}{2}\rho(x,t)V^2\, d\tau &= \frac{1}{2}\frac{\partial}{\partial t}\left(q_m^2(t)\int_{x_1}^{x_2}\frac{\rho(x,t)}{q_m^2(t)}\left(\int_{S(x)} V^2 d\sigma\right)dx\right) \\
&= \frac{1}{2}\frac{\partial}{\partial t}\left(q_m^2(t)\int_{x_1}^{x_2}\frac{\rho(x,t)}{\rho(x,t)^2 S(x)}\frac{1}{S(x)\overline{V}^2(x,t)}\left(\int_{S(x)} V^2 d\sigma\right)dx\right) \\
&= \frac{1}{2}\frac{\partial}{\partial t}\left(q_m^2(t)\int_{x_1}^{x_2}\frac{\beta(x,t)}{\rho(x,t)S(x)}dx\right) \\
&= \frac{1}{2}\frac{\partial}{\partial t}\left(q_m^2(t)f(t)\right) \qquad (4)
\end{aligned}$$

with :

$$f(t) = \int_{x_1}^{x_2}\frac{\beta(x,t)}{\rho(x,t)S(x)}dx \qquad (5)$$

and

$$\beta(x,t) = \frac{1}{S(x)\overline{V}^2(x,t)}\int_{S(x)}\overrightarrow{V}^2(x_i,y,z,t)d\sigma \qquad (6)$$

The function $f(t)$ depends on the shape of the pipe, on the shape of the velocity profile and also on density $\rho(x,t)$.

The dimensionless number $\beta(x,t)$ characterizes the momentum distribution in the section pipe $S(x)$ at the instant t (i.e. momentum coefficient or shape factor of the velocity profile).

Kinetic energy flux (II) throught $S_1 \cup S_2$:

The term (II) of the Eq. (2) can be expressed in terms of the mass flow rate $q_m(t)$:

$$\begin{aligned}
\int_{S_1\cup S_2}\frac{1}{2}\rho V^2(\overrightarrow{V}.\overrightarrow{n})d\sigma &= \int_{S_2}\frac{1}{2}\rho(x_2,t)\overline{V}^3(x_2,y,z,t)d\sigma - \int_{S_1}\frac{1}{2}\rho(x_1,t)\overline{V}^3(x_1,y,z,t)d\sigma \\
&= \frac{1}{2}\rho(x_2,t)\alpha(x_2,t)S_2\overline{V}^3(x_2,t) - \frac{1}{2}\rho(x_1,t)\alpha(x_1,t)S_1\overline{V}^3(x_1,t) \\
&= \frac{q_m^3(t)}{2}\left(\frac{\alpha(x_2,t)}{\rho(x_2,t)^2S_2^2} - \frac{\alpha(x_1,t)}{\rho(x_1,t)^2S_1^2}\right) \qquad (7)
\end{aligned}$$

with :

$$\alpha(x_i,t) = \alpha_i(t) = \frac{1}{S_i \overline{V}^3(x_i,t)} \int_{S_i} \overrightarrow{V}^3(x_i,y,z,t)d\sigma \tag{8}$$

and $$\rho(x_i,t) = \rho_i(t) \tag{9}$$

thus :

$$\int_{S_1 \cup S_2} \frac{1}{2}\rho V^2 (\overrightarrow{V}.\overrightarrow{n})d\sigma = \frac{q_m^3(t)}{2}\left(\frac{\alpha_2(t)}{\rho_2(t)^2 S_2^2} - \frac{\alpha_1(t)}{\rho_1(t)^2 S_1^2}\right) \tag{10}$$

The dimensionless number $\alpha_i(t)$ characterizes the distribution of kinetic energy in section S_i at instant t (i.e. kinetic energy coefficient or shape factor of the kinetic energy profile).
It plays the same role as the $\beta(x,t)$ coefficient for the shape of the momentum profile.

Power of pressure forces (III) :

Using again the definition of the mass flow rate $q_m(t)$ in term (III) of the Eq. (2), yields:

$$\begin{aligned}
\int_{S_1 \cup S_2} p(\overrightarrow{V}.\overrightarrow{n})d\sigma &= p(x_2,t)\int_{S_2} \overline{V}(x_2,t)d\sigma - p(x_1,t)\int_{S_1} \overline{V}(x_1,t)d\sigma \\
&= p(x_2,t)\overline{V}(x_2,t)S_2 - p(x_1,t)\overline{V}(x_1,t)S_1 \\
&= q_m(t)\left(\frac{p(x_2,t)}{\rho(x_2,t)} - \frac{p(x_1,t)}{\rho(x_1,t)}\right)
\end{aligned} \tag{11}$$

thus :

$$\int_{S_1 \cup S_2} p(\overrightarrow{V}.\overrightarrow{n})d\sigma = q_m(t)\left(\frac{p_2(t)}{\rho_2(t)} - \frac{p_1(t)}{\rho_1(t)}\right) \tag{12}$$

with :

$$p(x_i,t) = p_i(t) \tag{13}$$

Power of the external viscous stress (V):

$$\int_{\partial\mathcal{D}} \overrightarrow{\tau}.\overrightarrow{V}\ d\sigma = \int_{S_1\cup S_2} \overrightarrow{\tau}.\overrightarrow{V} d\sigma = P_{vs}(t) \tag{14}$$

Without moving walls, the power of external viscous forces exerted on the $S_1 \cup S_2$ border of the $\mathcal{D}$ domain are summed up by the power of the viscous stress on the sections S_1 and S_2. Often negligible when compared to the power of pressure forces.

Power dissipated by viscosity (VI) :

$$\int_{\mathcal{D}} \phi_1 d\tau = P_{v\mathcal{D}}(t)$$

The power $P_{v\mathcal{D}}(t)$ dissipated in $\mathcal{D}$ by viscosity is *a priori* negligible compared to other terms (parallel flow) except in the cases where fluids undergo shear stress in $\mathcal{D}$ (e.g. meet an obstacle, a grid, a porous material) as will be seen further on.

Finally:

$$\begin{aligned}\frac{1}{2}\frac{\partial}{\partial t}\left(q_m^2(t)f(x,t)\right) + \frac{q_m^3(t)}{2}\left(\frac{\alpha_2(t)}{\rho_2(t)^2 S_2^2} - \frac{\alpha_1(t)}{\rho_1(t)^2 S_1^2}\right) \\ = q_m(t)\left(\frac{p_1(t)}{\rho_1(t)} - \frac{p_2(t)}{\rho_2(t)}\right) + P_{vs}(t) - P_{v\mathcal{D}}(t)\end{aligned}$$

2.3.1. Additional assumptions:

1. In case of fully-developed flows (i.e. whose velocity profile shape, but not amplitude, remains the same at all times), it may be admitted that shape factors α and β are independent of time.
2. If, in addition, we consider only turbulent flows or entrance regimes (i.e. the velocity is uniformly distributed over the pipe width), the shape factors α and β are uniform and (the thickness to the boundary layers close) are equal to one. Thus:
   $\overrightarrow{V}(x,y,z,t) = V(x,y,z,t)\overrightarrow{x} = V(x,t)\overrightarrow{x} \quad ; \quad \rho(x,y,z,t) = \rho(x,t).$
   For pulsating flow, as soon as the frequency exceeds a few Hz, the velocity profile remains constant over the pipe diameter (with the exception of boundary layers of course), regardless of the mean flow. This point is detailed in Appendix A.

3. Except in special cases, the terms (V) and (VI) are negligible. More on this point in the section 2.4.

Taking into account these additional assumptions, a simplification is obtained:

$$\frac{1}{2}\frac{\partial}{\partial t}\left(q_m^2(t)f(x,t)\right) + \frac{q_m^3(t)}{2}\left(\frac{1}{\rho_2^2 S_2^2} - \frac{1}{\rho_1^2 S_1^2}\right) = q_m(t)\left(\frac{p_1(t)}{\rho_1(t)} - \frac{p_2(t)}{\rho_2(t)}\right) \quad (15)$$

with:

$$f(x,t) = \int_{x_1}^{x_2} \frac{1}{\rho(x,t)S(x)}dx$$

Note that the function $f(t)$ contains $\rho(x,t)$ and will therefore be constant only if the compressibility effects are negligible. If gas density is assumed not to vary between positions 1 and 2, $\rho(x,t) = \rho(t)$:

$$f(t) = \int_{x_1}^{x_2} \frac{1}{\rho(x,t)S(x)}dx = \frac{1}{\rho(t)}\int_{x_1}^{x_2} \frac{1}{S(x)}dx = \frac{1}{\rho(t)}A \quad \text{with : } A = \int_{x_1}^{x_2} \frac{dx}{S(x)}$$

and

$$\frac{df(t)}{dt} = -\frac{A}{\rho(t)^2}\frac{d\rho(t)}{dt}$$

the different terms of Equation (15) are then written:

$$\begin{aligned}
(I) \qquad & \tfrac{1}{2}\tfrac{d}{dt}\left(q_m^2(t)f(t)\right) && = q_m\frac{dq_m(t)}{dt}f(t) + \frac{1}{2}q_m^2(t)\frac{df(t)}{dt} \\
(II) \qquad & \tfrac{q_m^3(t)}{2}\left(\tfrac{1}{\rho_2(t)^2 S_2^2} - \tfrac{1}{\rho_1(t)^2 S_1^2}\right) && = \frac{q_m^3(t)}{2\rho(t)^2}\left(\frac{1}{S_2^2} - \frac{1}{S_1^2}\right) \\
& && = \frac{q_m^3(t)}{\rho(t)^2}B \quad \text{with : } B = \frac{1}{2}\left[\frac{1}{S_2^2} - \frac{1}{S_1^2}\right] \\
(III) \qquad & q_m(t)\left(\tfrac{p_1(t)}{\rho_1(t)} - \tfrac{p_2(t)}{\rho_2(t)}\right) && = \frac{q_m(t)}{\rho(t)}\left(p_1(t) - p_2(t)\right) = \frac{q_m(t)}{\rho(t)}\Delta P(t)
\end{aligned}$$

The equation (15) becomes :

$$\begin{aligned}
& q_m\tfrac{dq_m(t)}{dt}\tfrac{1}{\rho(t)}A - \tfrac{1}{2}q_m^2(t)\tfrac{A}{\rho(t)^2}\tfrac{d\rho(t)}{dt} + \tfrac{q_m^3(t)}{\rho(t)^2}B && = \frac{q_m(t)}{\rho(t)}\Delta P(t) \\
\Leftrightarrow \qquad & \tfrac{dq_m(t)}{dt}A - \tfrac{1}{2}q_m(t)\tfrac{A}{\rho(t)}\tfrac{d\rho(t)}{dt} + \tfrac{q_m^2(t)}{\rho(t)}B && = \Delta P(t)
\end{aligned}$$

2.3.2. Taking into account the reversal of the flow direction:

When the direction of the flow is reversed (e.g. intake of combustion engine) the preceding equations must be re-written because they come from global balance equations related to the reference frame (1-D flow and one direction $\overrightarrow{x}$). To take this into account in the kinetic energy term (II), thus:

$$\frac{dq_m(t)}{dt}A - \frac{1}{2}q_m(t)\frac{A}{\rho(t)}\frac{d\rho(t)}{dt} + \frac{q_m(t)|q_m(t)|}{\rho(t)}B = \Delta P(t) \qquad (16)$$

$$\text{with :} \quad A = \int_{x_1}^{x_2} \frac{dx}{S(x)} \quad \text{and} \quad B = \frac{1}{2}\left[\frac{1}{S_2^2} - \frac{1}{S_1^2}\right]$$

It is a much simpler and more natural method than the method used by Werner *et al.*[14] to calculate the bidirectional flow from the stationary Bernoulli equation.

2.3.3. Cases of incompressible fluids:

As long as the flow velocity is not too high (i.e. $Ma < 0,3$) the flow can be considered as incompressible and the density ρ is only a function of local temperature and static pressure. The Eq. (16) becomes:

$$A\frac{dq_m(t)}{dt} + B\frac{q_m(t)|q_m(t)|}{\rho(t)} = \Delta P(t) \qquad (17)$$

$$\text{with :} \quad A = \int_{x_1}^{x_2} \frac{dx}{S(x)} \quad \text{and} \quad B = \frac{1}{2}\left[\frac{1}{S_2^2} - \frac{1}{S_1^2}\right]$$

An ordinary nonlinear differential equation (ODE) is obtained that it looks like the unsteady Bernoulli equation. It is simple enough to be computed in real-time, that is to say in less than one time step. The two constants A and B depend only on the geometry of the device and are therefore known *a priori*: There is no calibration to perform.

The flow measurement is deduced from the pressure drop induced by the Venturi (the flow velocity is different between the inlet and the outlet of the control volume), but the total energy carried by the fluid is conserved. It is assumed that head loss due to the friction in the control volume is negligible, which is true over a wide range of flow rates. To gain precision it is possible to estimate the head loss and take it into account in the flow rate computation

but it will be significant only for high flow rate and increases the computation time.

The principle require a fully developed flow profile and so this device is sensitive to disturbed flow conditions. The flowmeter should be inserted as far away as possible from any flow disturbances with a inlet length (and outlet if there is backflow) of at least 10 diameters.

Attention must be paid to the change of direction of the flow (backflow), which for a too high flow rate, would cause separation of the flow from the wall. The equation (17) would no longer be valid and the measurements would be wrong. This principle of measurement with a pressure drop induced by a Venturi is therefore only relevant without backflow or for reverse flow rate very small.

2.3.4. Example of an application to the intake of a combustion engine:

Fig. 2 shows an example of unsteady flow rate measured at the intake of a 2.0 L four-cylinder combustion engine at 2271 rpm. It is compared with the mean flow measured by a reference mass flowmeter placed in series.

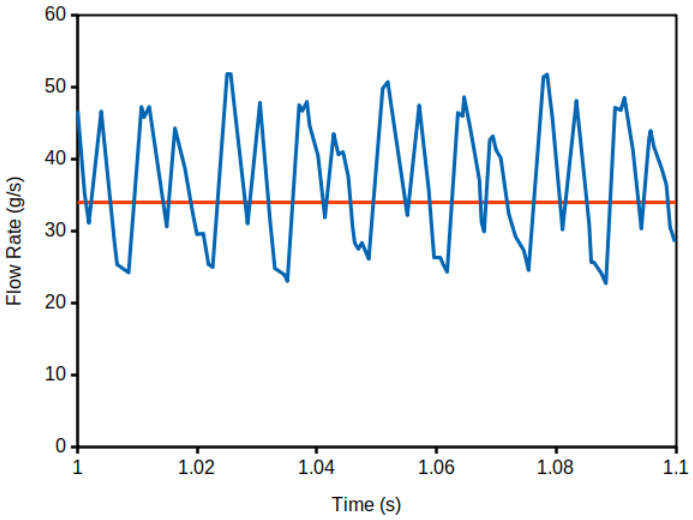

Fig. 2. Example of unsteady flow rate at the intake of a 2.0 l 4-cylinder combustion engine at 2271 RPM. Comparison between unsteady prototype flow meter (blue) and reference mass flowmeter (red) : mean Flow Rate = 34 ± 2 g/s.

2.4. Control volume with a singularity:

A control volume is defined as shown in Fig. 3, consisting of a right circular cylinder of diameter D inside which is placed a grid (for example). Eq. (2) always applies and each of its terms written as previously except terms (II) and (VI).

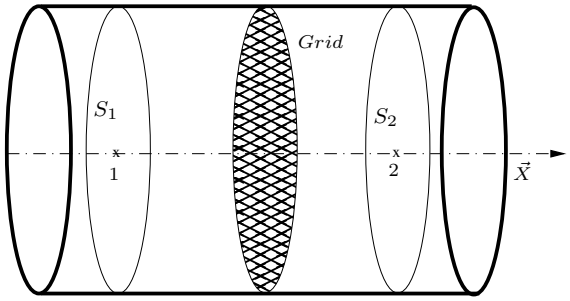

Fig. 3. Control volume consisting of a right circular cylinder with $\vec{x}$ axis and cross section $S_i(x)$.

Kinetic energy flux (II) throught $S_1 \cup S_2$:

If the inlet cross section S_1 and outlet S_2 are equal, the term (II) is then zero.

Viscosity dissipation (VI) :

It has been assumed previously that the power dissipated by viscous friction $P_{v\mathcal{D}}(t)$ in domain $\mathcal{D}$ of Venturi type control volume is usually negligible in front of the other terms. This is not the case if the fluid undergoes shear stress within the bulk, for example in the case where the fluid passes through a grid or a porous material. The integral of the dissipation rate in $\mathcal{D}$ is usually defined by the product of the head loss $\Delta\xi$ and the volumetric flow rate q_v:

$$\int_{\mathcal{D}} \phi_1 d\tau = \Delta\xi \times q_v(t) = \Delta\xi \times \frac{q_m(t)}{\rho} \quad \text{wiyh} \quad \Delta\xi = \Lambda \frac{1}{2} \rho \overline{V}^2$$

hence:

$$\int_{\mathcal{D}} \phi_1 d\tau = \frac{q_m(t)^3}{\rho^2} C \quad \text{with} \quad C = \Lambda \frac{8}{\pi^2 D^4}$$

The constant C is the coefficient of head loss due to the singularity, it must be determined experimentally (or the dimensionless friction factor Λ).

The equation (15) becomes :

$$\frac{1}{2}\frac{\partial}{\partial t}\left(q_m^2(t)f(x,t)\right) + \frac{q_m^3(t)}{\rho^2}C = q_m(t)\left(\frac{p_1(t)}{\rho_1(t)} - \frac{p_2(t)}{\rho_2(t)}\right)$$

With the same assumptions as previously, it is coming for an incompressible fluid:

$$A\frac{dq_m(t)}{dt} + C\frac{q_m(t)|q_m(t)|}{\rho} = \Delta P(t) \tag{18}$$

$$\text{with :} \quad A = \int_{x_1}^{x_2} \frac{dx}{S(x)} \quad \text{and} \quad C = \Lambda\frac{8}{\pi^2 D^4}$$

Here again, an ordinary nonlinear differential equation (ODE) is obtained sufficiently straightforward to be computed in real-time, in the sense that all computations can be done in less than one time step and the flow rate obtained in less than 100 μs for an acquisition frequency of 10 kHz. The explicit Euler method, for example, provides sufficient precision while not requiring much computing time. The precision of a higher order Euler scheme would be obtained at the expense of the calculation time.

The flow measurement is deduced from the pressure drop due to the singularity introduced into the pipe and, unlike the Venturi, it is energy dissipated in the form of heat and thus lost for flow.

However, this device with a grid to create the pressure drop is much less sensitive to the disturbed flow conditions than the Venturi device.

The constant A depends only on the geometry of the device and is therefore known *a priori*. On the other hand, the constant C (or the friction factor Λ) must be determined beforehand, this configuration consequently requires a calibration of the flowmeter prototype.

2.4.1. Calibration:

The device causing the pressure drop, must be calibrated according to the maximum flow rate to be measured and the range of the differential pressure sensor.

A prototype of unsteady flowmeter was built with a grid to produce the pressure drop. It consists of a cylindrical pipe of diameter $D = 63$ mm provided with a square mesh grid (Stainless Steel Wire, mesh square 1 mm, wire

diameter 0.3 mm), a differential pressure sensor (FirstSensor, HCL series, range ±2500 Pa, calibrated and temperature compensated) , a K-type thermocouple with 1.5 probe diameter and static pressure sensors (FirstSensor, HMA series, range ±100 hPa) for estimating the flow density $\rho(t)$. The differential pressure sensor is positioned near the grid, the pressure taps are separated by a distance equal to the half pipe diameter on both side of the grid.

This flowmeter prototype is placed in a steady flow in series with a reference mass flowmeter (Proline t-mass Endress+Hauser, maximum measured error ±1.5%). The pressure loss coefficient C was determined for the two flow regimes: transition and turbulent (c.f. Fig. 4).

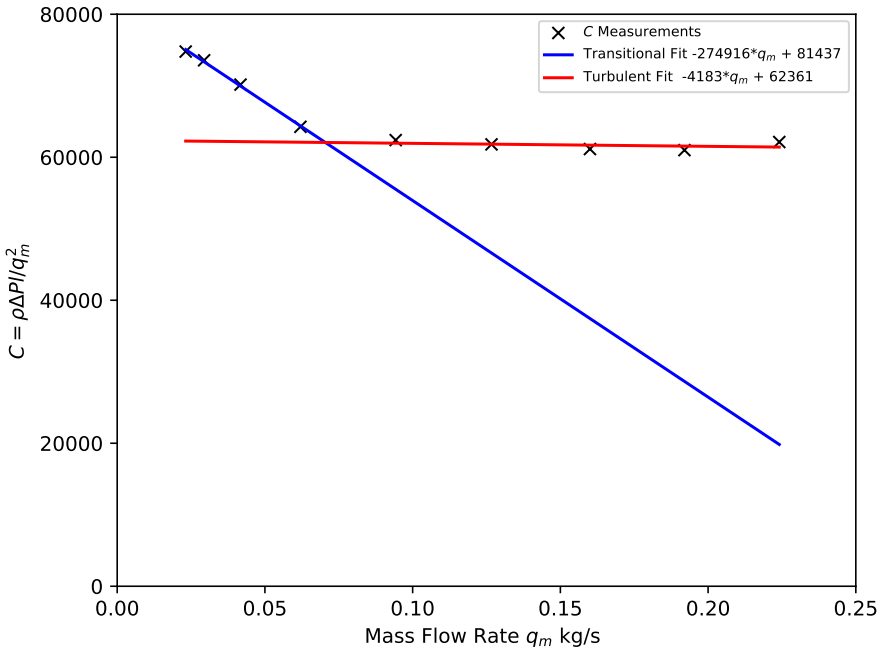

Fig. 4. Calibration curves of flowmeter prototype. Coefficient $C = \rho\Delta P/q_m^2$

.

2.4.2. Example of pulsating flow at the intake of a driven single-cylinder combustion engine:

An example of the unsteady flow rate measured at the intake of a driven single-cylinder engine of 0.5 litre is shown in the Fig. 5. The unsteady flowmeter and the reference mass flowmeter are placed in series immediately upstream of the cylinder head and the intake is done at atmospheric pressure. The figure shows that the flow is strongly pulsated and changes direction several times per period. The unsteady flowmeter prototype tracks flow fluctuations even when it changes direction. The mean flow rate given by the reference flowmeter is 7.3 g/s while the unsteady measurements provided by the prototype, and integrated over a whole number of periods, gives 7.46 g/s, that is to say barely 2.2% difference.

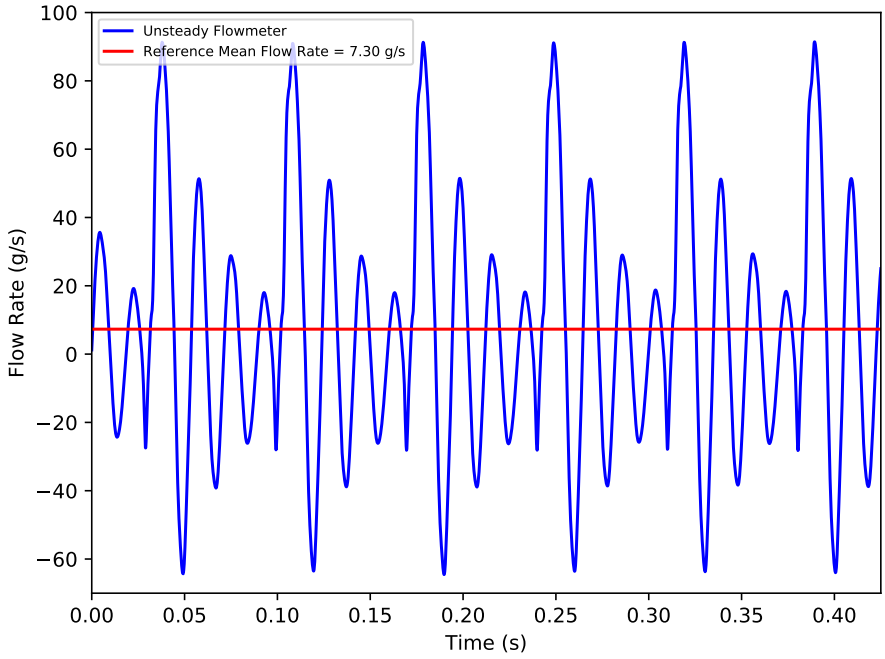

Fig. 5. Unsteady flow rate at the inlet of a single-cylinder combustion engine electrically driven at 1709 rpm.

3. Results and Discussion:

A particular care must be taken in the differential pressure measuring chain by a remote sensor.

3.1. Bandwidth of the differential pressure measurement system:

The bandwidth of the system must be as wide as possible and in all cases wider than the double of the higher frequency of the unsteady flow to be measured according to the Shannon's theorem (at least larger than the double of the the frequencies that carry the most energy). This bandwidth must also be as flat as possible despite the resonances that can appear in the whole data chain acquisition of the differential pressure (orifice, connecting tube and pressure sensor), as explained for example in Doblhoff-Dier *et al.*[9]. An anechoic termination of the connection tubes allow to significantly extend the flat part of the spectral bandwidth of the differential pressure sensor.

The remote pressure probes (i.e. differential pressure sensor, connecting tube 0.8 mm inner diameter and 15 cm long) are frequency calibrated by comparison to 1/4" GRAS type BP40 microphone. For this both measuring systems are connected in a coupler crossed by a pressurized jet of air used as acoustic source. The phase measurement (c.f. Fig. 6) allow to estimate the group delay to a little less than 0.8 ms ($-d\phi/d\omega = 0.77$) for the $0 - 400$ Hz frequency band. The bandwidth was also examined and compared with the bandwidth of a device with an anechoic termination added to the connecting tube.

Fig. 7 shows that the bandwidth of the system is significantly improved by the anechoic termination and that at up to 400 Hz it remains flat, which goes well beyond the 200 Hz that can be considered as the main target for combustion engines applications.

3.2. Unsteady flow rate at the intake of a combustion engine:

It is difficult to evaluate the accuracy of measurements of a device that is the only one that can provide them.There are mainly three systems that can be used to estimate an unsteady flow in a pipe. It is possible to use a Hot Wire Anemometer and then integrate the local velocity measurement on the section of the pipe. However, the hot wire is intrusive and can not be used when the flow velocity is less than about 5 m/s (it induces convection which is not negligible when the flow velocity is low) but moreover it is not sensitive in the velocity direction and therefore the measurements are rectified when

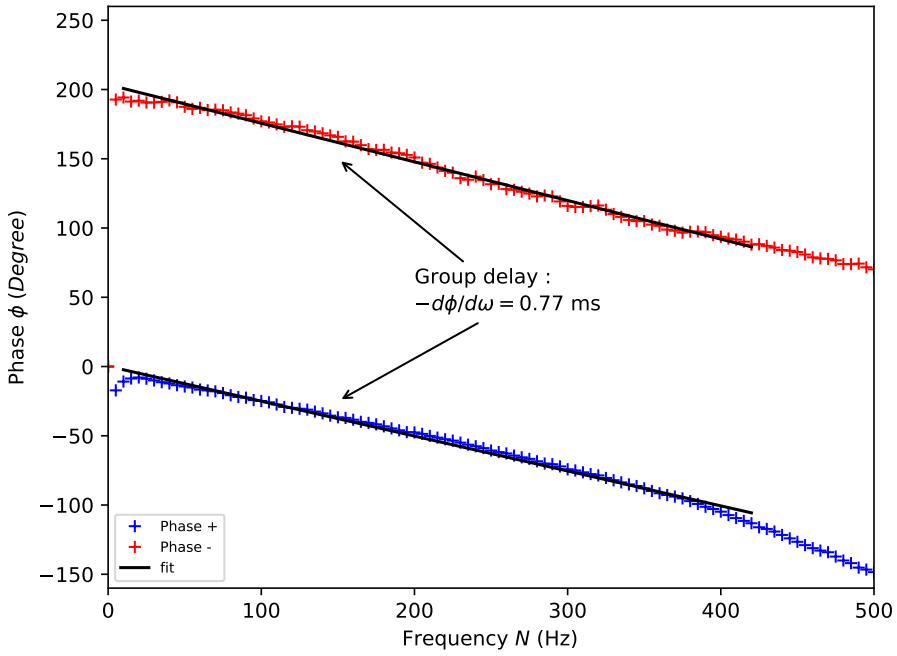

Fig. 6. Phase and Group-Delay of the remote differential pressure sensor

the direction of the flow is reversed (in case of backflow). It is therefore not a reference measurement.

-It is also possible to use Laser Doppler Velocimetry (LDV). As the Hot Wire Anemometer it provides an almost local measurement of the flow velocity, which must be then integrated on the section of the pipe to obtain flow rate. In addition it is necessary to seed the flow with particles and the measurements are not well time resolved (the velocity is measured only when particle passes through the measurement volume). The accuracy of flow measurement by LDV is not easy to estimate; it is therefore not a reference measurement.

Measurements by Particle Image Velocimetry (PIV) are also possible but they impose constraining optical accesses and, as with the LDV, it is necessary to seed the flow with particles and then to integrate the velocity field onto the section of the pipe. The measurements are not very well time resolved and their accuracies are not easy to estimate; it is still not a reference measurement.

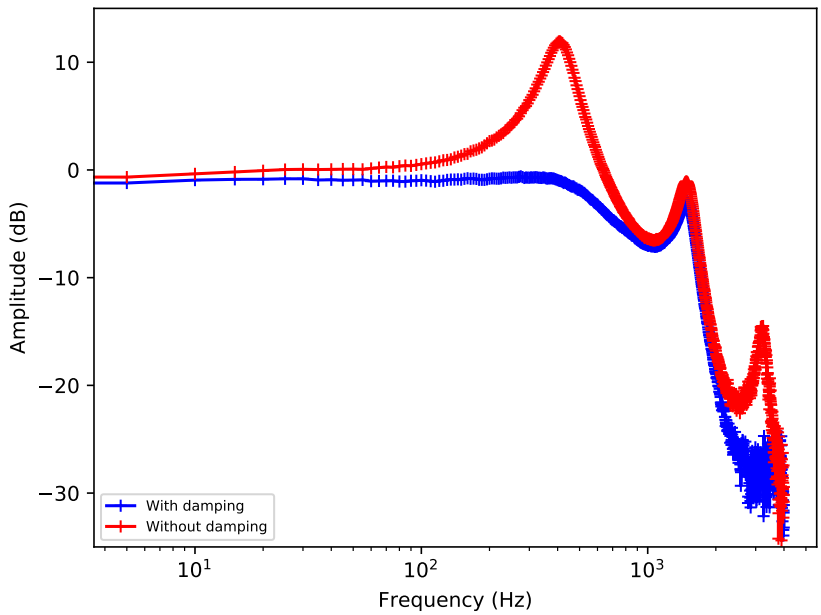

Fig. 7. Frequency response of remote differential pressure sensor, with and without damping.

On the other hand there are several devices allowing with a good accuracy to measure mean flow rate.The choice was made to compare the results obtained by our device averaged in time with the mean flow measurements given by Thermal Mass Flowmeter.

Two examples of unsteady flow rates measured at the intake of a three-cylinder combustion engine are shown below.

Fig. 9 and 10 show measurements obtained with a rotational speed of 1200 rpm and 2500 rpm, respectively. The sampling frequency was 10 kHz. It can be seen that in this configuration the rate of pulsation is much lower than on the single-cylinder and there is no longer any backflow. It can be noted that the convergence time of the flow rate computation is about 40 ms for 1200 rpm and 25 ms for 2500 rpm, about half a period.

As explained above, the accuracy of experimental results is difficult to evaluate, as it is difficult to establish the unsteady flow by other means in order to obtain a meaningful comparison. However results presented here

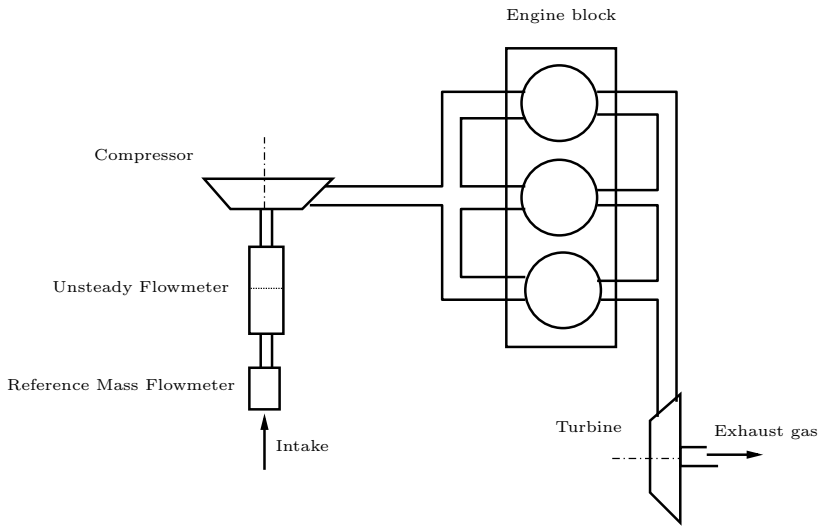

Fig. 8. Scheme of the experimental setup

show good agreement with the mean flow rate. The expected mean flow rate is 12.5 g/s for 1200 rpm while the unsteady measurements provided by the prototype and integrated over a whole number of periods gives 11.46 g/s. The difference is slightly less than 9%, but the mean flow measured by the thermal reference flowmeter on the engine test stand is not accurate to more than 5% . For the 2500 rpm case, the expected mean flow rate is 33.6 g/s while the unsteady measurements integrated over a whole number of periods gives 31 g/s.

3.3. Response time:

The nonlinear ODE equations (17) & (18) on which the device is based can be seen as "low-pass filters". It is therefore useful to examine the step response of these equations. The following figure Fig. (11) shows the response of equation (18) to steps of different amplitudes. It shows that the response time of the system is shorter as the amplitude of the excitation increased. The response time is defined as the moment when 99% of the step amplitude is reached.

Fig.(12) is a zoom of Fig.(10) with response of equation (18) to a step of 31.08 equal to the mean flow rate measured. It can be seen that the convergence time of the unsteady flowmeter towards the mean flow rate corresponds to the response time of equation (18). The response time of the

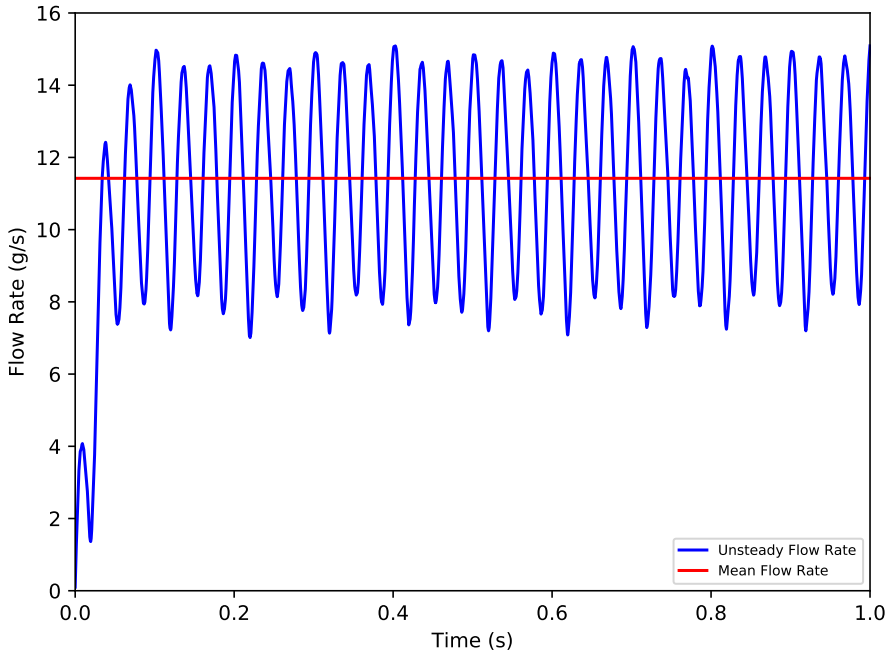

Fig. 9. Unsteady flow rate at the intake of a 3 cylinders engine of 1.2 litre; torque 80 Nm at 1200 rpm.

device is therefore mainly due to the behavior as a low-pass filter of equation (18).

4. Conclusion

Two methods in order to measure unsteady flow rate in real time (that is to say in less than one time step) from a differential pressure in a pipe were presented. Both methods are based on two similar nonlinear ordinary differential equations obtained from the equation kinetic energy balance.

The first method gives the unsteady flow rate from the pressure drop measured at a Venturi throat. It is demonstrated that there is no calibration to perform (except eventually for the differential pressure sensor) because the two constants in the ODE depend only on the geometry of the device and then known *a priori*. The principle requires a fully developed flow profile and so this device is sensitive to disturbed flow conditions. The flowmeter should

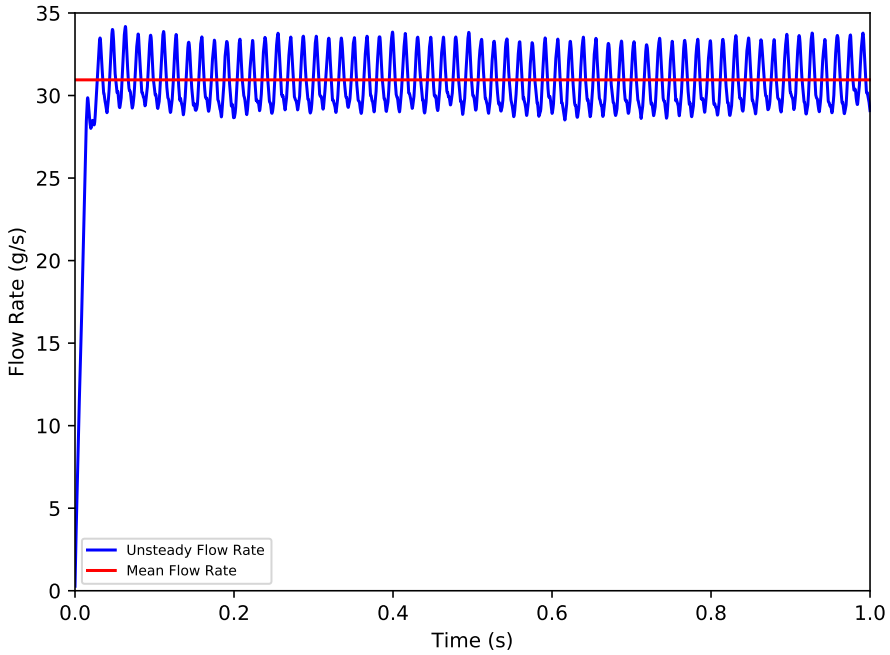

Fig. 10. Unsteady flow rate at the intake of a 3 cylinders engine of 1.2 litre; torque 120 Nm at 2500 rpm.

be inserted as far away as possible from any flow disturbances with a inlet length (and outlet if there is backflow) of at least 10 diameters. However this method is mainly relevant without backflow or for small reversed flow rate to avoid separation.

-The second method is based on a nonlinear ordinary differential equation similar to the former one but one of the two constants in the ODE must be determined experimentally. The flow measurement is deduced from the pressure drop due to a grid introduced into the pipe (or similar singularity); unlike the first method (Venturi throat), this device with a grid is clearly less sensitive to the disturbed flow conditions. The device causing the pressure drop, must be calibrated according to the maximum flow rate reached in the pipe and according to the range of the differential pressure sensor.

A prototype of unsteady flowmeter was built on this principle and calibrated with a steady flow and a reference mass flowmeter. The remote differential pressure measurement must be performed with care. The bandwidth

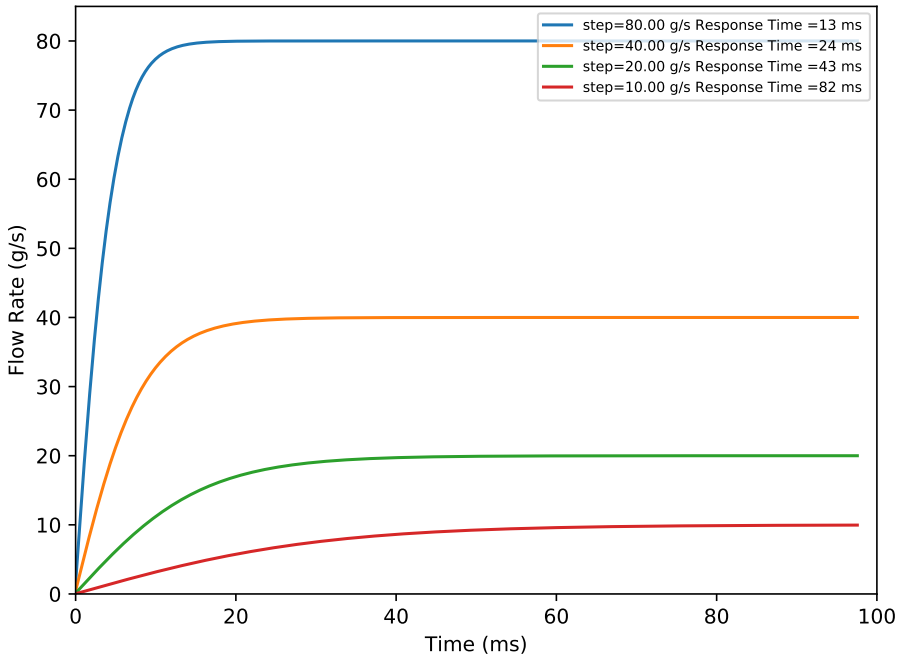

Fig. 11. Step Response of equation (18).

of the system is founded significantly improved by an anechoic termination and remains flat up to 400 Hz which is broadly sufficient for the targeted applications, the intake or exhaust of combustion engines. It has been shown that the convergence time of the device is shorter as the amplitude of the excitation increased, according to the behaviour of a low-pass filter of the ODE.

-The accuracy of experimental results is challenging to evaluate, as it is difficult to measure unsteady flow by other means in order to obtain a meaningful comparison. However results obtained show good agreements with unsteady measurements integrated over a whole number of periods and reference mass flowmeter.

The presented device and methodology yield adequate performances for the combustion engine application context.

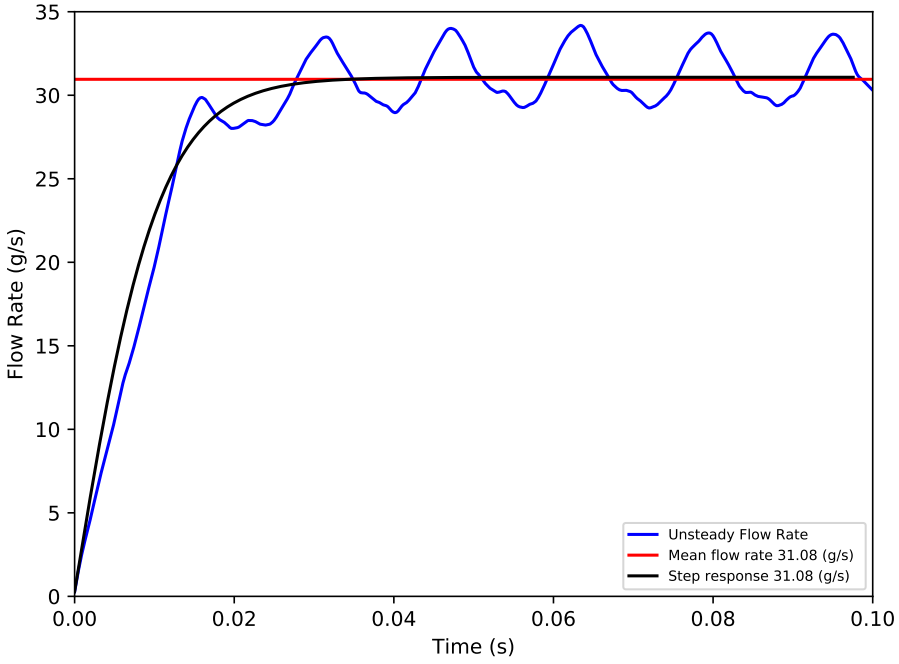

Fig. 12. Zoom of Fig. (10); comparison with Step Response of equation (18).

Appendix A. Pulsating laminar flow in pipe

The error made on the mean flow rate measurement of a oscillatory flow by neglecting the boundary layers can be estimated. Consider laminar and incompressible flow in a circular cylindrical pipe. The flow is generated by a periodic pressure gradient in the longitudinal direction $\frac{\partial p}{\partial x} = \Re\left[a_0 exp(j\omega t)\right]$. Numbers of authors (e.g. : [15, 16]) have shown that there is an exact solution of this problem with Bessel functions of order 0.

$$u(r,t) = \frac{a_0}{4\nu}(R^2 - r^2) + \Re\left\{\frac{a_1 R^2}{j\nu\alpha^2}\left[1 - \frac{J_0(\alpha r/Rj^{3/2})}{J_0(\alpha j^{3/2})}\right]e^{j\omega t}\right\}$$

The first term of the right-hand side is the Poiseuille solution for a permanent flow with a constant longitudinal pressure gradient a_0. It is easy to deduce the flow rate $U_0 = \frac{a_0 R^2}{8\nu}$.
The second term of the right-hand side corresponds to a periodic solution of zero mean flow. The relation between the inertial effects due to pulsatile flow frequency and the viscous effects is defined by the dimensionless number first proposed by Lambossy [17] but known as Womersley number: $\alpha = R\sqrt{\frac{\omega}{\nu}}$ (where $\omega = 2\pi N$ (rad/s) is the angular velocity). It denotes the phase lag between pressure gradient and flow. When α is small (1.32 or less [18]), the frequency of pulsations is sufficiently low that a parabolic velocity profile has time to develop during each cycle, thus the flow will be very nearly in phase with the pressure gradient. When α is large (10 or more), the velocity profile is relatively flat or plug-like and the mean flow lags the pressure gradient by about 90 degrees. However, when the flow is turbulent (Re over 2300), the time-averaged velocity profile in pipes remains approximately flat even if the Womersley Number is relatively small.

To get an idea, figure A.13 shows the velocity profile of a pulsed laminar flow at the same frequency as the flow rate measured at the inlet side of a single-cylinder engine driven at 1709 rpm(c.f. figure (5)).

Computed velocity profiles are plotted for different values of the phase angle $\in [-180°, 180°]$. The phase shift between the boundary layers and the center of the pipe is clearly noticeable, as is the flat profile in much of the field.

In conclusion, for most applications considered, for example the air loop of combustion engines, the velocity is constant in most of the pipe. The error committed by neglecting the boundary layers will remain very small, either

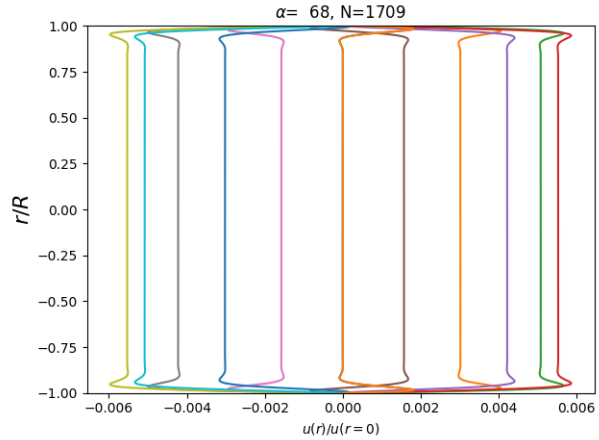

Fig. A.13. Laminar pulsated flow in pipe. Theoretical computation.

because the flow pulsations are relatively high ($\alpha > 10$) or because the flow is turbulent ($Re > 2300$).

References

[1] Gajan P, Mottram R, Hebrard P, Andriamihafy H and Platet B 1992, The influence of pulsating flows on orifice plate flowmeters, Flow. Meas. Instrum. 3(3), (1992), 118 – 129.

[2] Bokhorst E V and Peters M C A M Optimisation of flow measurements in a pulsating flow-experiences from field measurements. 19th International North Sea Flow Measurement Workshop 22-25 October 2001, Kristiansand, Norway.

[3] Laurantzon F, Örlü R, Tillmark N and Alfredsson P H, (2012), Response of common flowmeters to unsteady flow, Technical Report.

[4] Durst F, nsal B, Ray S and Trimis D (2007), Method for defined mass flow variations in time and its application to test a mass flow rate meter for pulsating flows, Meas. Sci. Technol,**18** (2007), 790-802.

[5] Ray SS, nsal BB, Durst FF, Ertunc , Bayoumi OA. Mass Flow Rate Controlled Fully Developed Laminar Pulsating Pipe Flows. ASME. J. Fluids Eng. (2005), 127(3):405-418.

[6] Foucault, E., Szeger, P., Laumonier, J., and Micheau, P., (2009), Unsteady Flow Meter, Brevet n° WO2005080924A1, U.S. Patent No. 7,519,483 B2.

[7] Foucault E., Szeger P., Laumonier J. and Micheau P., (2007), Real-time Non-stationary Flowmeter, Brevet n° WO2009118290A1 : Real Time Non-Stationary Flow Meter.

[8] A. Beaulieu, E. Foucault, P. Braud, P. Micheau and P. Szeger, A flowmeter for unsteady liquid flow measurements, Flow Measurement and Instrumentation, (2011), vol 22, 1, 131-137.

[9] Doblhoff-Dier K., Kudlaty K., Wiesinger M. and Grschl M., Time resolved measurement of pulsating flow using orifices, Flow Meas. Instrum., (2011), 22, 97 – 103.

[10] Reis M. N. and Hanriot S., Incompressible pulsating flow for low Reynolds numbers in orifice plates, Flow Meas. Instrum., (2017), 54, 146 – 157.

[11] Johnston N, Pan M, Kudzma S, Wang P. Use of Pipeline Wave Propagation Model for Measuring Unsteady Flow Rate. ASME. J. Fluids Eng. 2014;136(3):031203-031203-8.

[12] C. Bon, Relation pression-vitesse d'une classe d'écoulement instationnaire : application à la mesure des débits instantanés, Université de Poitiers, (1996), PhDThesis.

[13] Peube J-L., Fundamentals of Fluid Mechanics and Transport Phenomena, ISTE, (2009), Wiley USA.

[14] Werner, M., Baar, R., Haluska, P., and Sandor, I. (2016). Bidirectional flow measurement based on the differential pressure method for surge analysis on a small centrifugal compressor. Proceedings of the Institution of Mechanical Engineers, Part C: Journal of Mechanical Engineering Science.

[15] Womersley J R Method for the calculation of velocity, rate of flow and viscous drag in arteries when the pressure gradient is known. The Journal of Physiology, (1955) 127, 553–563.

[16] Uchida S., The pulsating viscous flow superposed on the steady laminar motion of incompressible fluid in a circular pipe. Zeitschrift für angewandte Mathematik und Physik ZAMP, (1956), 7, 403–422.

[17] LAMBOSSY P., Oscillations forcées d'un liquide incompressibile et visqueux dans un tube rigide et horizontal. Calcul de la force frottement, Helv. Physica Acta, (1952), 25 371–386.

[18] Çarpinlioğlu M.Y. and M. Y. Gündoğdu, A critical review on pulsatile pipe flow studies directing towards future research topics, Flow Meas. Instrum., (2001), 12, 163 – 174.